Open Access Full Text Article

ORIGINAL RESEARCH

Decoding the Intercellular Cross-Talking Between Immune Cells and Renal Innate Cells in Diabetic Kidney Disease by Bioinformatics

Meng Zhou*, Fang Lu*, Ling Jiang, Chen Chen, Si Chen, Luhan Geng, Rui Sun, Qing Li, Suyan Duan, Bo Zhang, Huijuan Mao, Changying Xing, Yanggang Yuan

Department of Nephrology, the First Affiliated Hospital of Nanjing Medical University, Nanjing Medical University, Nanjing, People's Republic of China

*These authors contributed equally to this work

Correspondence: Yanggang Yuan; Changying Xing, Department of Nephrology, The First Affiliated Hospital of Nanjing Medical University, Jiangsu Province Hospital, 300 Guangzhou Road, Nanjing, Jiangsu Province, 210029, Tel/Fax +86-25-6830-6462, Email ygyuan@njmu.edu.cn; cyxing62@126.com

Aim: Diabetic kidney disease (DKD) continues to be devastating complication of diabetes mellitus. Immune response and inflammatory reaction play essential roles in the progression of DKD. But the specific mechanism of immune cells, and their act on renal innate cells remains unclear. This article focused on immune cells and their communication with renal innate cells to provide bioinformatic evidence for further understanding the immune mechanism in DKD.

Methods: Data were analyzed to evaluate the differentially expressed genes (DEGs) and their pathways in DKD patients and mice. Gene set enrichment analysis (GSEA) was used to explore the immune inflammation-related pathways. CIBERSORT was applied to evaluate the distribution of inflammatory cells in different states. Cell-type DEGs and their enrichment pathways were further explored in podocytes, proximal tubule cells and injured tubule cells. Cellchat was used to reveal the cellular communication between immune cells and renal innate cells in DKD.

Results: GO and KEGG analysis showed that DEGs were mainly enriched in immune inflammation-related pathways. Monocytes, M2 macrophages and T cells were significantly increased in DKD samples, especially in renal tubule. ScRNA datasets showed that the immune cells number in DKD were significantly increased. Cell-type DEGs were involved in kidney growth and development. In DKD, the interaction numbers and strength between immune cells and innate cells were significantly increased. VISTANT, SPP1 and IGF signal flow were increased in DKD. SPP1-CD44, NRG1-ERBB4, NAMPT-INSR, and Igf1-Igf1r receptor ligand pairs were enhanced in DKD, which mediated the communication between immune-inflammatory cells and innate cells.

Conclusion: Our study explored the pathogenesis of renal injury promoted by immunoinflammatory in DKD. VISTANT, SPP1, and IGF signaling pathways and SPP1-CD44, NRG1-ERBB4, NAMPT-INSR, and Igf1- Igf1r receptor ligand pairs might occupy essential place in the occurrence and progress of DKD.

Keywords: diabetic kidney disease, immune cells, renal innate cells, bioinformatics

Introduction

The incidence of diabetes mellitus (DM) and its medical and social pressures have become a global burden and is expected to increase to 48% by 2045.[1] As one of the most serious microvascular complications of DM, diabetic kidney disease (DKD) remains as the most common cause of end-stage renal disease (ESRD) in developed world, notably in the elderly population.[2,3] Traditional renal injury hypothesis includes glomerular hyperperfusion, hyperpressure, and hyperfiltration.[4] In addition, compensatory aggravation of renal glucose load, change of renal hemodynamics, and effect of cytokines and genetic factors contribute to the pathogenesis of DKD.[5–7] Conventional therapies and molecular-based targeted inhibitors or antagonists, such as sodium-glucose cotransporter (SGLT2) inhibitor, have been proved to delay the progression of DKD. However, many DKD patients still gradually progress to ESRD.[8] Therefore, more effective

treatments targeting the pathogenesis of DKD at the cellular, molecular and genetic levels need to be meticulously explored.

Numerous genes have been found to be associated with the pathogenesis, progression, or prognosis of DKD. The vital role of inflammatory reaction and immune response of immune cells in DKD has been gradually discovered currently. For example, Jia Y et al identified that vascular cell adhesion molecule 1 (VCAM1) was an immune-related hub gene in DKD. VCAM1 expression was significantly elevated in patients with DKD accompanied by the increased expression of various immune cells and was inversely correlated with the glomerular filtration rate (GFR).[9] However, the essential role of immune cells and relevant pathways in DKD with the specific potential mechanism needs to be explained. The continuous development of bioinformatics, especially the substantial application of single-cell sequencing technology, allows us to interpret the pathogenesis of DKD from a more precise and targeted perspective.

By analyzing four human and mice datasets, including Microarray, snRNA-seq, and scRNA-seq data, this study aimed to explore the inflammatory mechanism and crosstalk between immune cells and renal innate cells in DKD and search for signaling pathways or receptor ligand pairs that might play a vital role in DKD pathogenesis or serve as potential biomarkers and therapeutic targets for early detection and treatment of DKD.

Materials and Methods
Data Acquisition and Processing
Microarray, snRNA-seq, and scRNA-seq data were downloaded from the Gene Expression Omnibus (GEO) database (http://www.ncbi.nlm.nih.gov/geo). The GSE30528 dataset included data on glomeruli samples from patients with 9 DKD and 13 healthy controls on the GPL571 platform (Affymetrix Human Genome U133A 2.0 Array). The GSE30259 dataset contained data on renal tubular tissues from patients with 10 DKD and 12 healthy controls on the GPL571 platform (Affymetrix Human Genome U133A 2.0 Array). The snRNA-seq data from patients with 3 DKD and 3 healthy controls were obtained from the GSE131882 dataset on GPL24676 (Illumina NovaSeq 6000 (Homo sapiens)). ScRNA-seq data from 5 ob/m mice and 6 db/db mice were obtained from the GSE184652 on GPL24247 (Illumina NovaSeq 6000 (Mus musculus)). For the datasets in GSE30528 and GSE30529, the "Affy"[10] package in R (https://www.r-project.org/) software was used to perform background correction and normalization. For scRNA-seq and snRNA-seq data, "DoubletFinder" was used to remove the potential doublets.[11] "Seurat"[12] was used to standardize the expression of filtered samples and identify the top 2000 genes with the most noticeable difference between cells. Cells were filtered out with the threshold of the ratio of mitochondrial genes ≤5% and ribosomal genes ≥10%. Genes expressed in >3 cells and cells with at least 500 genes were retained. An integrated dataset was created by using the data integration method (Harmony).

Dimensionality Reduction and Cell Annotation
The integrated data then proceeded with principal component analysis (PCA), and the dimensions of the top 30 PCs were reduced by the tSNE algorithm to obtain principal clusters. Finally, the cells were labeled and clustered according to their marker gene expression and the existing notes utilizing CellMarker.[13]

Differentially Expressed Genes (DEGs) Identification
The "limma"[14] package in R was used to identify the GSE30529 and GSE30528 datasets DEGs. For datasets GSE131882 and GSE184652, the FindMarkers function in Seurat was used to compare the gene expression between DKD and healthy control groups, with a significant FDR cutoff of 0.05 and log fold change of 0.5.

Gene Ontology (GO) and Kyoto Encyclopedia (KEGG) Enrichment Analyses
GO[15] and KEGG[16] pathway enrichment analyses of DEGs were conducted by the "clusterProfiler", "enrichplot", "org. Hs.eg.db", "org.Mm.eg.db" and "ggplot2" packages. $P < 0.05$ was considered statistically significant.

Gene Set Enrichment Analysis (GSEA)

The C5 (v7.5) gene set collections were downloaded from the Molecular Signatures Database v7.5 download page (https://www.gsea-msigdb.org/gsea/downloads.jsp). GSEA was performed based on the "clusterProfiler" packages. Only gene sets with P values of 0.05, |NES|>1, and FDR q-value <0.25 were considered significant.

Evaluation of Immune Cell Subtype Distribution

CIBERSORT was used to compare and analyze renal infiltrating immune cells between DKD and healthy control. The LM22 signature was used as the reference for 1000 permutations. The *P*-values and root mean squared errors were counted for each sample file in CIBERSORT. CIBERSORT *P* value was set at < 0.05. A matrix of immune cells fractions was generated. The visualization of the results from CIBERSORT was carried out using the R packages "ggpubr" and "ggplot2".

Cell-Cell Interaction Network Analysis

"CellChat" (v1.1.3) was used to infer the cell-cell interactions across different cell types by using the expression of known ligand-receptor pairs and identifying the changes in intercellular communications. For the analysis of the mice dataset, we used the precompiled mice Protein-Protein-Interactions as prior network knowledge and selected the "Secreted Signaling pathways" database. For the human dataset analysis, we also chose the "Secreted Signaling pathways" database and used the precompiled human protein–protein-Interactions as a priori network knowledge. Then, we compared the incoming and outgoing interaction numbers and strength of each pair of cell types to determine sending or receiving signals changes between DKD and control. The significant ligand-receptor pairs across comparisons were recognized by using the netVisual_aggregate, net_bubble, and netAnalysis_signalingRole_network functions in CellChat.

Immunohistochemical Analysis

The renal biopsy specimens of 24 DKD patients obtained from our center and 8 healthy control samples harvested from total nephrectomy of patients undergoing radical nephrectomy for renal cancer were examined. The kidneys were fixed in 4% paraformaldehyde, dehydrated, embedded into paraffin blocks, and sectioned at 3μm upon object slides, followed by deparaffinization, rehydration, antigen retrieval and incubation with specific primary antibodies at 4°C overnight. The following primary antibodies were used at a dilution of 1:500: SPP1 (osteopontin, Proteintech, 25,715-1-AP), CD44 (Proteintech, 15,675-1-AP), NAMPT (Visfatin, Proteintech, 11,776-1-AP), and INSR beta (Abcam, ab227831). The secondary antibody incubation and DAB staining were performed in the light of standard steps supplied by the manufacturer (MXB Biotechnologies, KIT-5920). Approximately 4 fields (×400 magnification) were randomly selected from each section for quantitative analysis. Image J software was used to analyze the integrated optical density (IOD).

Statistics

Pearson's correlation analysis between genes and GFR in DKD patients was performed using Nephroseq v5 online platform. The statistical analyses were carried out using R software and GraphPad Prism software. Statistical differences in more than 2 groups were identified by multiple comparisons with one-way ANOVA analysis. *P* value < 0.05 was deemed statistically significant.

Results

Identification of DEGs and Evaluation of Immune Cell Subtype Distribution

After standardization of the microarray results, a total of 453 DEGs were obtained from the GSE30528 dataset, including 130 upregulated and 323 downregulated genes (Figure 1A). Similarly, 380 upregulated and 86 downregulated DEGs were screened from the GSE30529 dataset (Figure 1B). The cluster heatmaps of the DEGs were shown in Figure 1C and D. We then used an intersection between DEGs in the GSE30528 dataset and GSE30529 for further analysis. As a result, a total of 102 upregulated and 14 downregulated DEGs were identified (Figure 1E). Using the CIBERSORT algorithm, the CD4 T cells, gamma delta T cells, resting mast cells, and M2 macrophage cells proportion were significantly increased in DKD
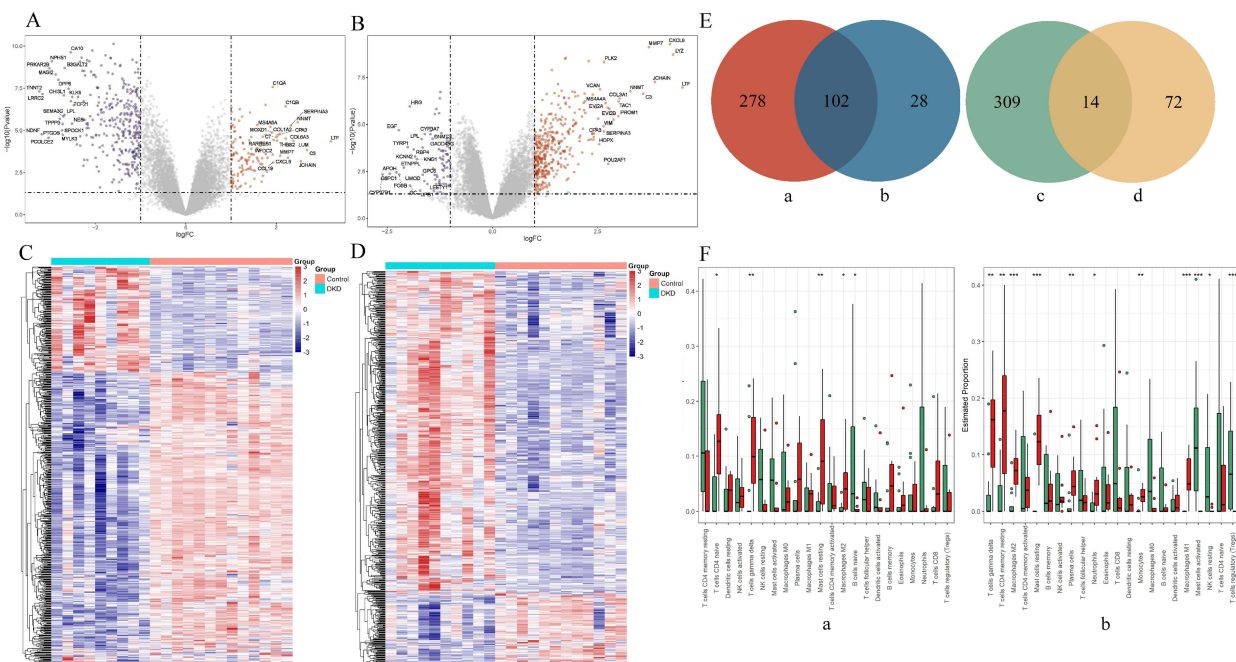
Figure 1 Different expression genes (DEGs) and immune cell type proportion in glom and tubule samples. (**A**). Volcano plots of DEGs in human renal glom dataset; (**B**). Volcano plots of DEGs in human renal tubule dataset; (**C**). The heatmap for DEGs in human renal glom dataset; (**D**). The heatmap for DEGs in human renal tubule dataset; (**E**). Venn diagram of common trend DEGs, a. up-regulated DEGs in renal tubule; b. up-regulated DEGs in renal glom; c. down-regulated DEGs in renal glom; d. down-regulated DEGs in renal tubule; (**F**). Different immune cell type proportion in DKD and Control, a: renal glom samples, b: renal tubule samples.

patients (*P*<0.05). Moreover, the proportion of these cell types was more evident in human tubule samples compared with healthy controls (Figure 1F).

For GSE131882 datasets, 12 clusters were identified, including proximal convoluted tubule cells (PCTs), injury proximal convoluted tubule cells (In. PCTs), a loop of Henle cells (LOH), distal convoluted tubule cells (DCTs), principal cells (PCs), intercalated cells (ICs), podocytes (PODOs), parietal epithelial cells (PECs), endothelium cells (ENDOs), mesangial cells (MES), and immune cells (Figure 2A). As a subset of PCTs, the In. PCTs were identified for expressing typical injury PCT markers, such as Havcr1, Vcam1, and C3. The immune cluster was extracted from the integrated dataset and subclustered into T cells, B cells, plasma cells, and monocytes (Figure 2B). In GSE184652 datasets, besides 12 clusters demonstrated above, there were other 6 clusters identified, including proximal straight tubule cells (PSTs), macular densa cells (MDs), juxtaglomerular apparatus cells (JGAs), the thick ascending limb cells (TALs), fibroblasts (Fibs) and descending thin limbs of Henle's loop cells (DTLs) (Figure 2C). Similarly, the immune cluster was subclustered into T cells, dendritic cells, and macrophages (Figure 2D). We further analyzed the cell type-specific DEGs in podocytes, PCTs, and In. PCTs. For the human snRNA dataset, 509 (380 up and 129 down), 5119 (4254 up and 865 down), and 1002 (633 up and 369 down) DEGs were identified in podocytes, PCTs and In. PCTs, respectively (Figure 3A–C). And for the mice scRNA dataset, 399 (229 up, 170 down), 311 (154 up, 157 down), and 468 (208 up, 260 down) DEGs were identified, respectively (Figure 3D–F).

GO, KEGG and Gene Set Enrichment Analyses

GO functional analysis indicated enrichment of the 116 DEGs in the GSE30528 and GSE30529 datasets, mainly including activation of the immune response, lymphocyte-mediated immunity, regulation of TNF production, T cell activation, mononuclear and cell proliferation pathway (Figure 4A). Furthermore, the complement and coagulation cascade system, cell adhesion molecules, ECM-receptor interaction, and PI3K-Akt signaling pathway were demonstrated by the KEGG pathway enrichment analysis (Figure 4B). In the GSE131882 human dataset, podocytes type-specific DEGs were mainly involved in the phosphate metabolic process (Figure 5A). PCTs type-specific DEGs were found to participate in the renal system, kidney development, and the carboxylic acid metabolic process (Figure 5B). The In. PCTs
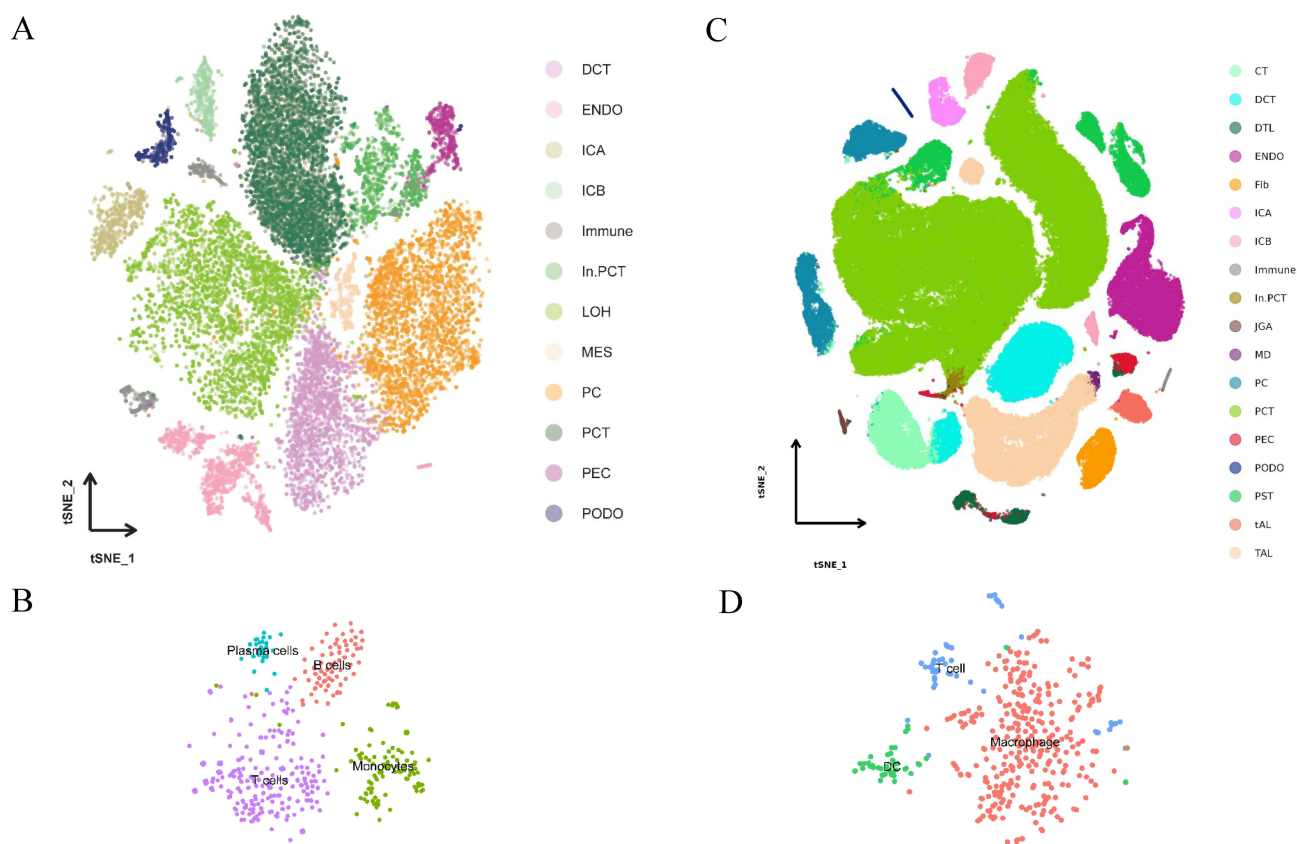
Figure 2 Integrated scRNA-seq dataset of diabetic and control samples. (**A**). T-distributed neighbor embedding (t-SNE) representation of cells from human snRNA-seq dataset; (**B**). The immune subsets extracted from human snRNA-seq dataset; (**C**). T-SNE representation of cells from mice scRNA-seq dataset; (**D**). The immune subsets from mice scRNA-seq dataset. Diabetic and control samples were integrated into a single dataset and clustered using Seurat.

Abbreviations: DCT, distal convoluted tubule; PCT, proximal convoluted tubule; In. PCT, injury proximal convoluted tubule cells; PC, principal cell; IC, intercalated cell; LOH, loop of Henle; CT, connecting tubule; CD, collecting duct; PODO, podocyte; ENDO, endothelium; MES, mesangial cell; Immune, immune cell; PST, proximal straight tubule cell; MD, macular densa cell; JGA, juxtaglomerular apparatus cell; TAL, thick ascending limb cell; DTL, descending thin limbs of Henle's loop cell; Fib, fibroblast.

type-specific DEGs were majorly involved in MAPK pathways, urogenital system and kidney development, and myeloid or leukocyte cell differentiation (Figure 5C).

Moreover, in the GSE184652 mice dataset, podocytes DEGs were mainly involved in the development of kidneys and regulation of cell adhesion (Figure 5D). DEGs of PCTs were involved in fatty acid, organic acid and carboxylic acid related metabolic processes (Figure 5E). However, compared with db/m mice, the In. PCTs DEGs of db/db mice participated in urogenital and renal system development and epithelial cell proliferation (Figure 5F). In addition, GSEA analysis indicated immune cell-related pathways such as T cell activation, differentiation, proliferation, and immune response pathways were enriched in three types of cells in human and mice datasets (Figure 6).

Cell Communication and Changes During Disease

To find out the specific patterns of intercellular interactions and changes during disease, we compared communication strengths and numbers by using CellChat between different immune cells and other kidney cell types, especially podocytes, PCTs, and In. PCTs. In human or mice datasets, under DKD conditions, the interaction numbers and strength between immune cells, especially macrophages, podocytes, PCTs, and In. PCTs were significantly increased (Figure 7A and B). We then estimated the relative information flow between DKD and control. For human data, NRG, BMP, SEMA3, GDF, CXCL, PDGF, CALCR, PROS, IL-16, CSF, ACTIVIN, GALECTIN, IGF, PTN and HGF information flow increased apparently in the DKD group (Figure 7C). In mice data, the information flow of FGF, SPP1, GALECTIN, CALCR and GDF pathways increased obviously in db/db group (Figure 7D). The specific genes involved in immune cells and innate cells were further analyzed in the two groups. In human DKD samples, VISFATIN, GALECTIN, and
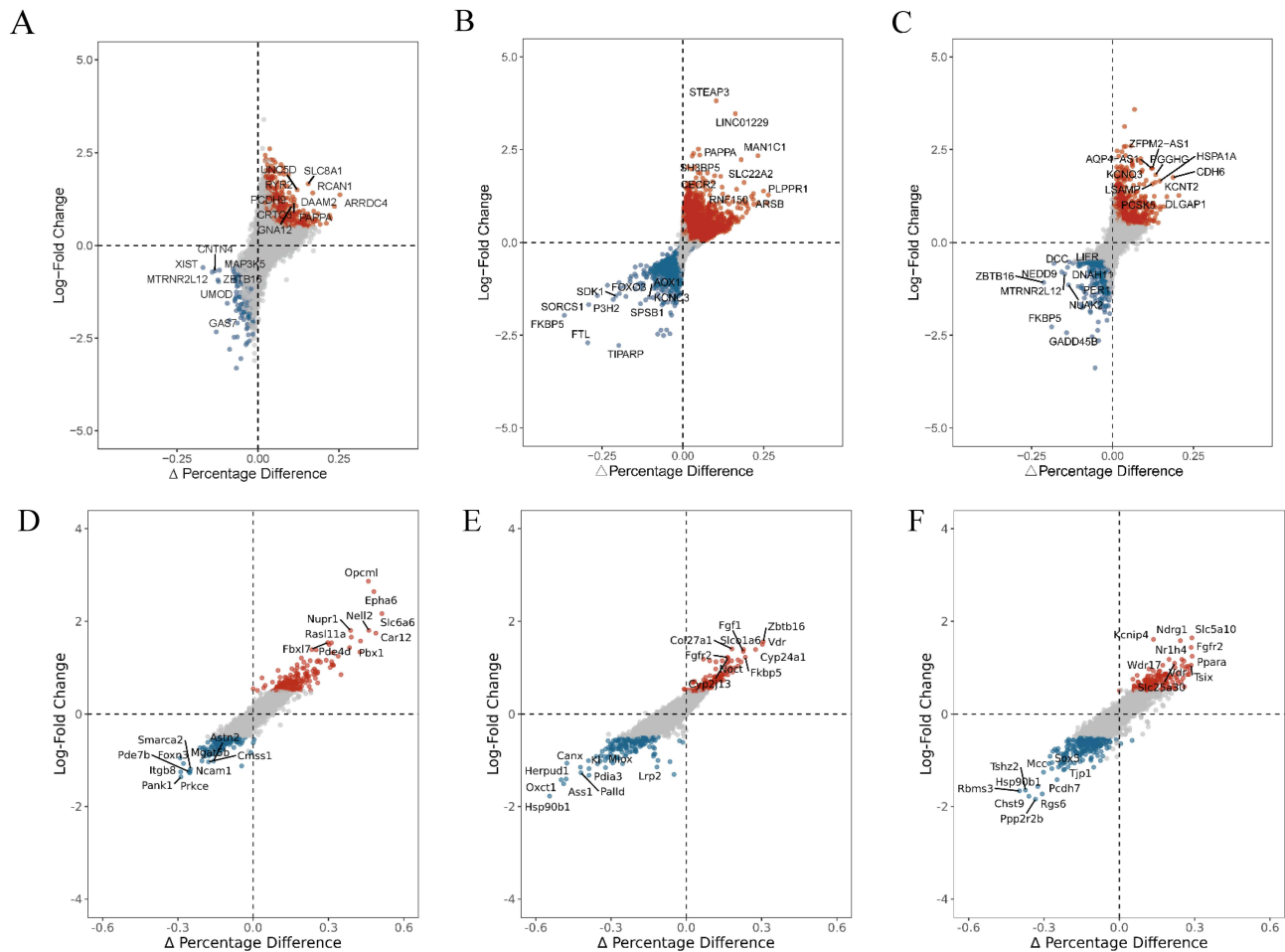
Figure 3 Different cell-type DEGs. (**A**). podocyte cell-type DEGs in human snRNA-seq dataset; (**B**). PCT cell-type DEGs in human snRNA-seq dataset; (**C**). In. PCT cell-type DEGs in human snRNA-seq dataset; (**D**). podocyte cell-type DEGs in mice scRNA-seq dataset; (**E**). PCT cell-type DEGs in mice scRNA-seq dataset; (**F**). In. PCT cell-type DEGs in mice scRNA-seq dataset. Differential gene expression analysis using the log-fold change expression versus the difference in the percentage of cells expressing the gene comparing DKD and control in podocytes, PCTs, and In. PCTs (Δ Percentage Difference). Gene labeled have log-fold change >0.5, Δ |Percentage Difference| >10%, and *P*-value from Wilcoxon rank sum test <0.05.

Figure 4 Functional enrichment analysis of common trend DEGs. (**A**) GO enrichment results of DEGs; (**B**). KEGG enrichment results of DEGs.
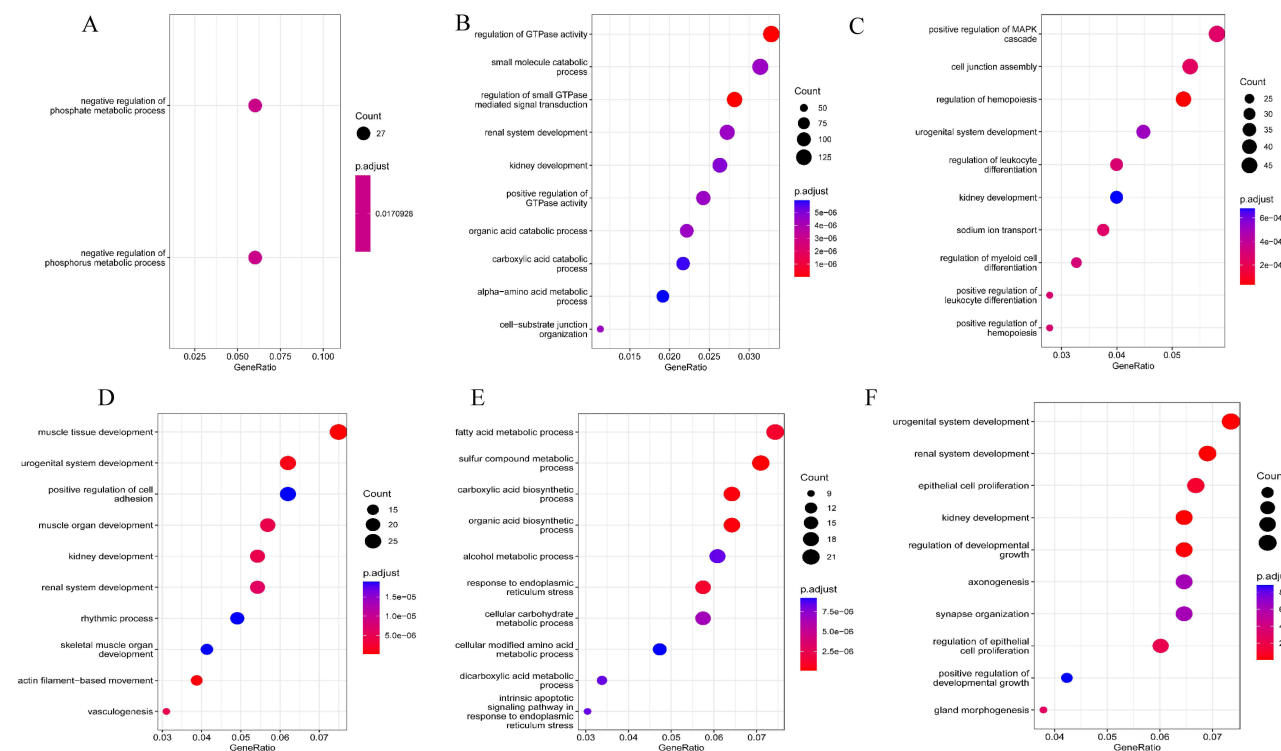**Abbreviations**: GO, Gene Ontology; KEGG, Kyoto Encyclopedia of Genes and Genomes.

Figure 5 GO biological process enrichment results of cell-type DEGs. The x-axis represents the gene ratio, and the y-axis represents the GO terms. (**A**). GO biological process enrichment results of podocyte cell-type DEGs in human snRNA-seq dataset; (**B**). GO biological process enrichment results of PCT cell-type DEGs in human snRNA-seq dataset; (**C**). GO biological process enrichment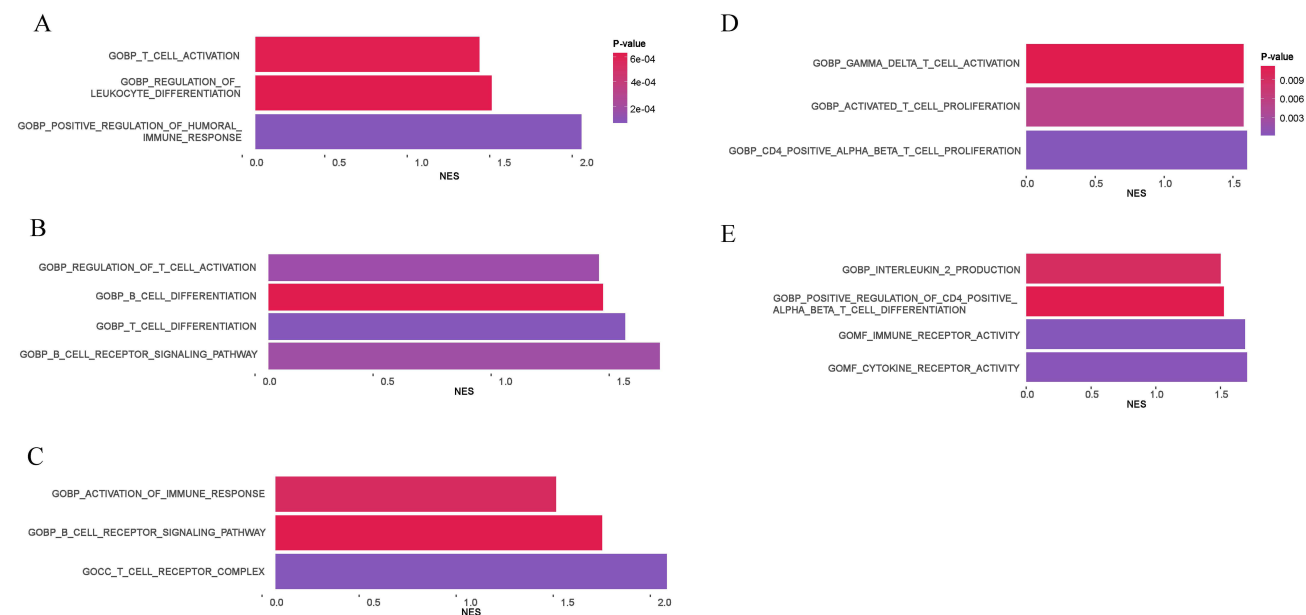 results of In. PCT cell-type DEGs in human snRNA-seq dataset; (**D**). GO biological process enrichment results of podocyte cell-type DEGs in mice scRNA-seq dataset; (**E**). GO biological process enrichment results of PCT cell-type DEGs in mice scRNA-seq dataset; (**F**). GO biological process enrichment results of In. PCT cell-type DEGs in mice scRNA-seq dataset.

Figure 6 Gene sets enrichment analysis (GSEA) results. (**A**). GSEA results of podocytes in human snRNA-seq dataset; (**B**). GSEA results of PCT in human snRNA-seq dataset; (**C**). GSEA results of In. PCT in human snRNA-seq dataset; (**D**). GSEA results of PCT in mice scRNA-seq dataset; (**E**). GSEA results of In. PCT in mice scRNA-seq dataset.

CSF signaling patterns increased in monocytes, with CXCL, IGF, and GALECTIN rising in T cells (Figure 8A). Meanwhile, in mice db/db samples, IGF, CSF, TGF-β, and GALCTIN signaling patterns increased in macrophages, with FGF, GDF, and GALECTIN rising in T cells (Figure 8B). Then we analyzed the up-regulated ligand-receptor pairs
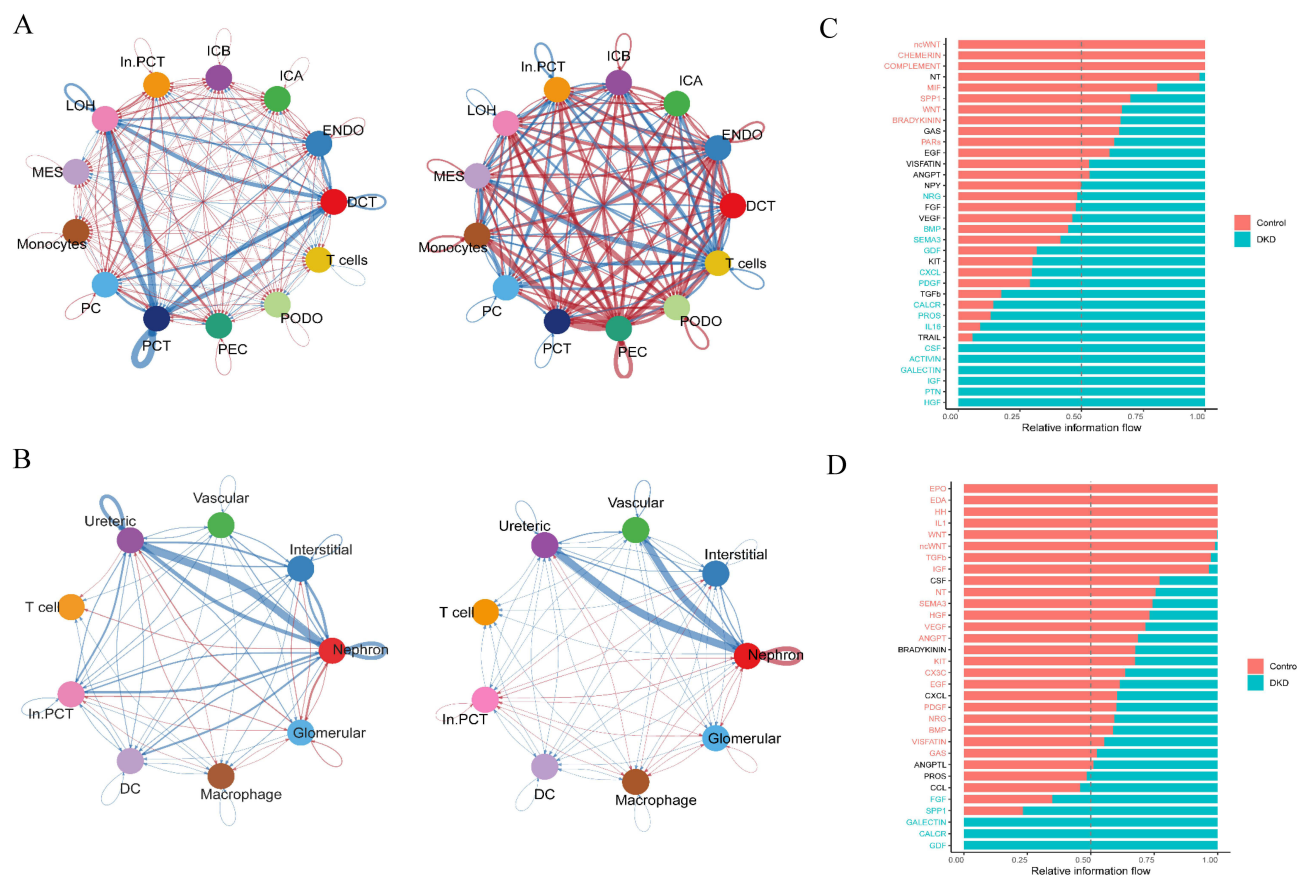
Figure 7 Changes in cell interaction number, strength under DKD condition and information flow. (**A**). Changes in cell interaction number and strength in DKD patients compared to healthy control, left: Differential numbers of interactions in human snRNA-seq dataset; right: Differential interactions strength in human snRNA-seq dataset; (**B**). Changes in cell interaction number and strength in DKD mice model: left: Differential numbers of interactions in mice scRNA-seq dataset; right: Differential interactions strength in mice scRNA-seq dataset; (**C**). Relative information flow in the human snRNA-seq dataset; (**D**). Relative information flow in mice scRNA-seq dataset. Nephron contains PEC, PCT, PST, In. PCT, DTL, TAL, MD, DCT; Ureteric contains CT, PC, ICA, ICB; Interstitial contains Fib, JGA; Glomerular contains PODO; Vascular contains ENDO. Red line: upregulated, blue line: downregulated. The thicker the line, the more significant the change.

under the DKD circumstance. In human samples, GDF15 and NRG1 were identified as secreted by In. PCTs signaling with monocytes and T cells. PLG and SPP1 secreted by PCTs signal with monocytes and T cells were also identified. Podocytes secreted NRG4, IGF, BTC, and BMP7 to communicate with immune cells (Figure 8C, left). From the immune cells point, monocytes tended to secret NAMPT and GAS6 to respond to PCTs, In. PCTs, and podocytes (Figure 8C, right). In mice samples, except Spp1 and Gdf15 secreted by the In. PCTs signaling with macrophages and T cells, Csf1 was also identified, whereas Sema3c and Gas6 were more obvious in PCTs. Furthermore, podocytes secreted Pros1, Il34, and Angptl2 to communicate with macrophages (Figure 8D, left). In response, macrophages secreted Nrg2 and Igf1 to interact with In. PCTs, PCTs, and podocytes (Figure 8D, right). Based on the change in information flow and up-regulated ligand-receptor pairs, we further analyzed the role of different cell types in all kinds of pathways under DKD and healthy conditions. Apparently, in the human dataset, the influencer role of monocytes was enhanced in VISFATIN, PROS, and GAS pathways. Instead, T cells acted as vital receivers in SPP1 and GDF pathways. More importantly, the sender role of monocytes in the VISFATIN pathway was obviously enhanced, and PCTs were the primary receiver (Figure 9A). For the mice dataset, the influencer role of macrophages was enhanced in IGF, GDF, and SEMA3 pathways. Notably, macrophages also played a crucial sender in IGF pathways (Figure 9B).

The Association Between Genes and Clinical Features of DKD

Correlation analysis and subgroup analysis between target genes and clinical features were conducted using the Nephroseq v5 online tool to verify the potential roles of genes illustrated above. First, the results showed that NRG1,
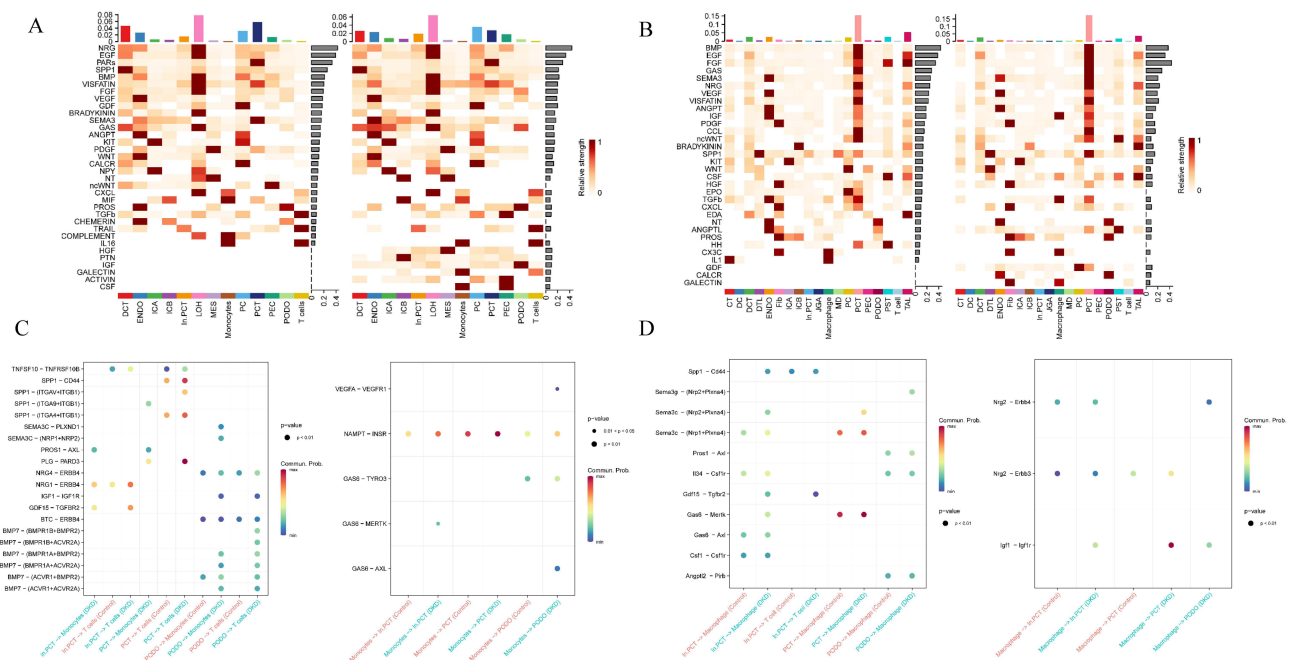
Figure 8 Upregulated information flow in different cell types and upregulated ligand-receptor pairs between immune and renal innate cell. (**A**) Upregulated information flow in different cell types in the human snRNA-seq dataset, left: Overall signaling patterns in control groups; right: Overall signaling patterns in DKD groups; (**B**) Upregulated information flow in the mice scRNA-seq dataset; left: Overall signaling patterns in control groups; right: Overall signaling patterns in DKD mice model groups; (**C**) Upregulated ligand-receptor pairs of DKD patients in human snRNA-seq datasets; left: Upregulated ligand-receptor pairs from innate cells to immune cells; right: Upregul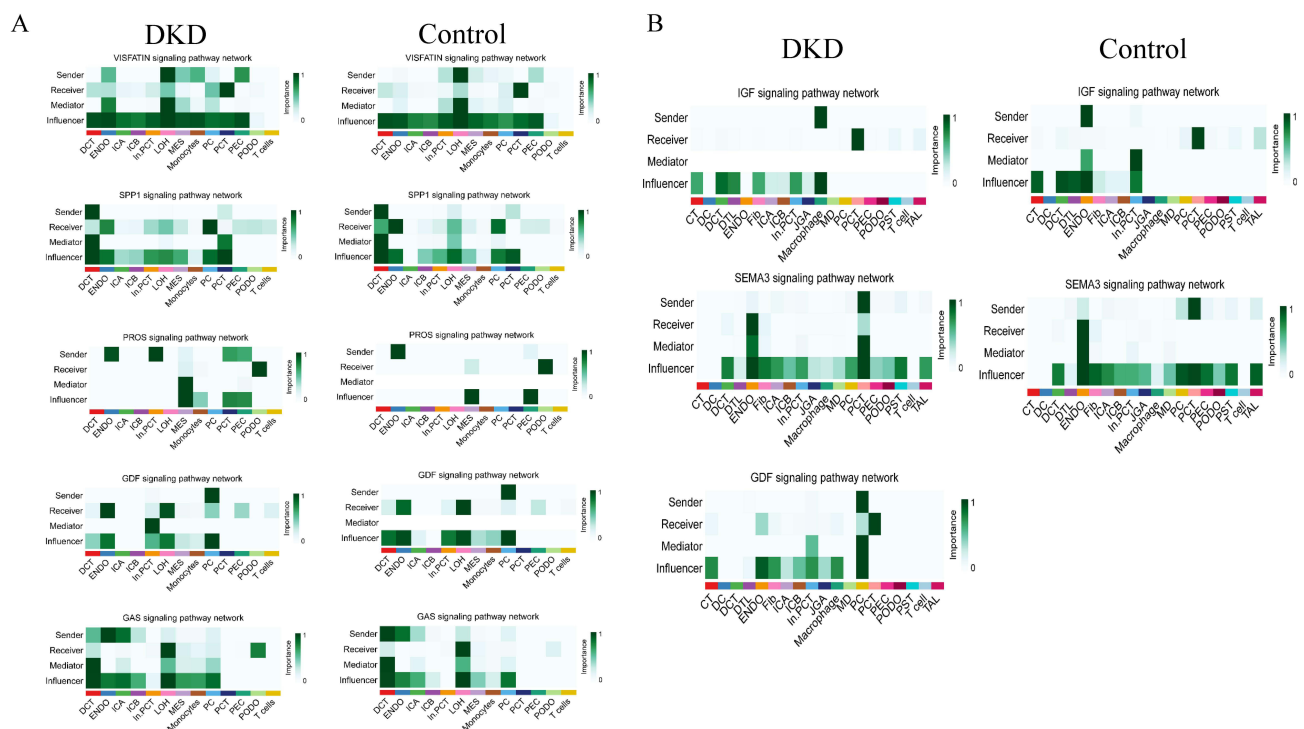ated ligand-receptor pairs from immune cells to innate cells; (**D**) Upregulated ligand-receptor pairs in the DKD mice model scRNA-seq dataset; left: Upregulated ligand-receptor pairs from innate cells to immune cells; right: Upregulated ligand-receptor pairs from immune cells to innate cells.

Figure 9 Different signaling pathways network and roles of different cells. (**A**) Different signaling pathways network in the human snRNA-seq dataset; (**B**) Different signaling pathways network in the mice scRNA-seq dataset.
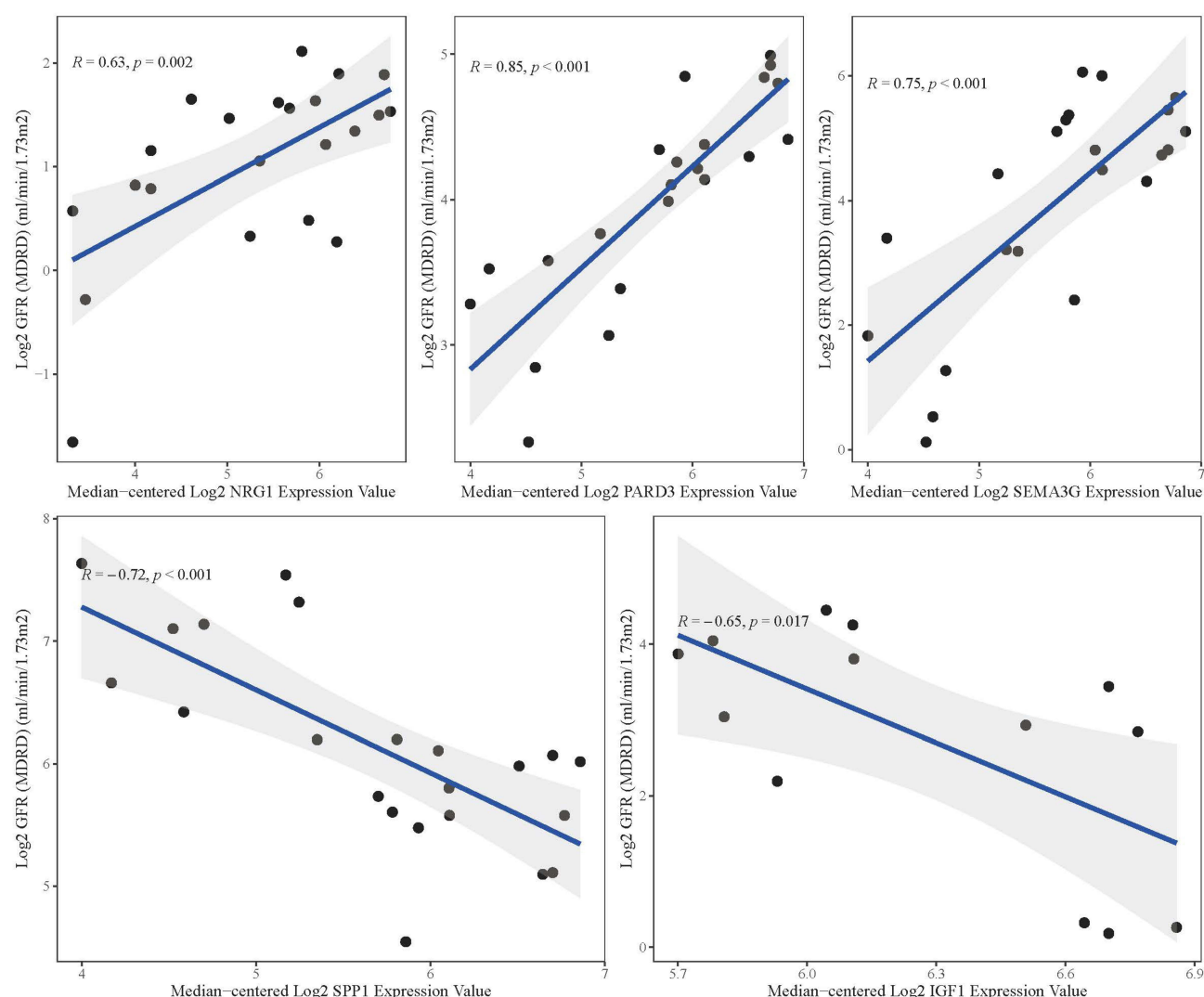
Figure 10 Related genes correlated with GFR.
Abbreviations: GFR, glomerular filtration rate; MDRD, modification of diet in renal disease; mRNA, messenger RNA.

PARD3, and SEMA3G mRNA expressions were positively related to GFR in DKD patients, indicating that these genes might have reno-protective effects. Meanwhile, SPP1 and IGF1 were negatively related to GFR in DKD patients, suggesting that these genes might deteriorate DKD progression (Figure 10). Immunohistochemical staining further verified the increased expression of SPP1 in renal PCTs and the increased expression of CD44 in the renal interstitium of DKD patients (Figure 11). The expression of another receptor ligand pairs NAMPT-INSR was also tested. Consisting with our bioinformatic prediction, the expression of NAMPT in renal interstitium was increased, accompanied by high expression of INSR in the innate cells (Supplement Figure 1).

Discussion

A total of 116 DEGs with common trends in microarray datasets were identified in glomeruli and tubule databases. GO enrichment analysis revealed DEGs were mainly enriched in immune-related pathways, such as T cell activation and immune response pathway, which implied the immune cell activation, migration, and response processes in DKD. These DEGs were also enriched in complement and coagulation cascades system, cell adhesion molecules, ECM-receptor interaction, and PI3K-Akt signaling pathway by KEGG enrichment analysis. We also found that the proportion of gamma delta T cells and M2 macrophages was significantly increased compared with the control groups in both renal tubules and
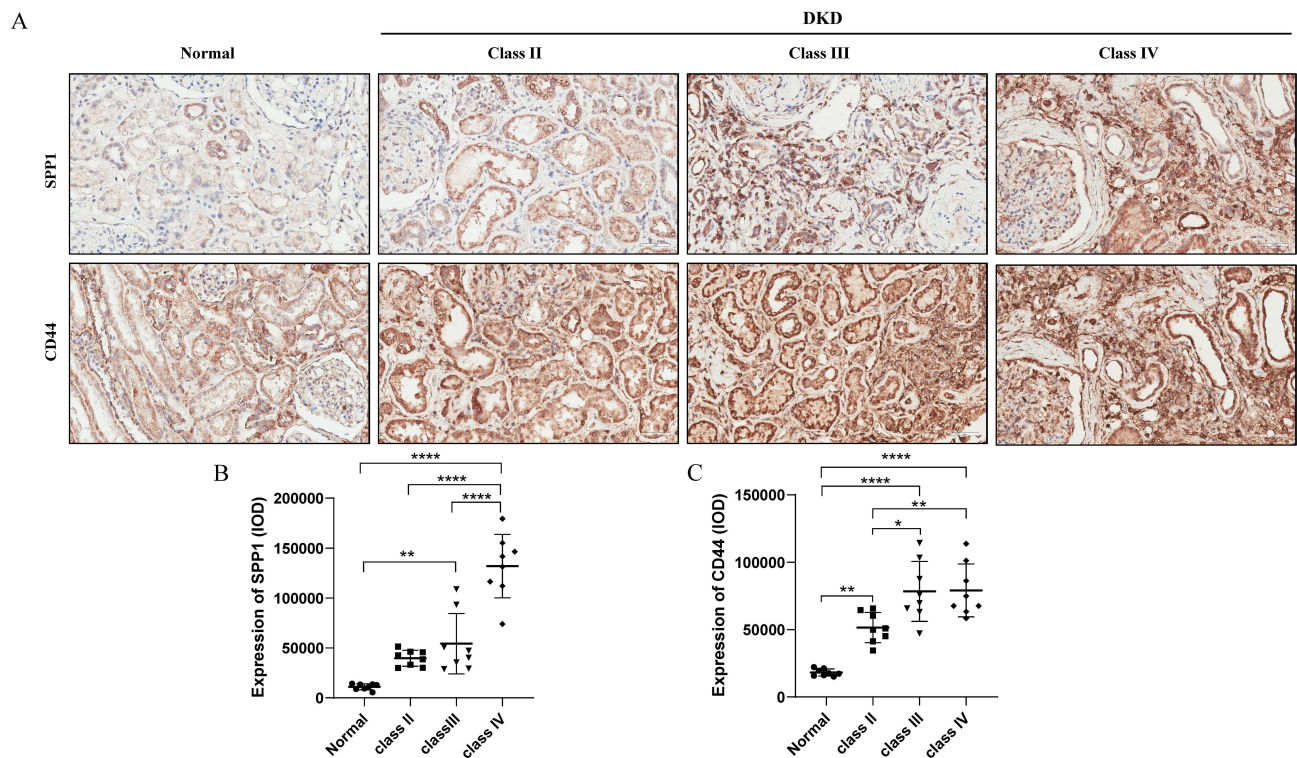
Figure 11 Expression of SPP1 and CD44 in renal tissues of healthy controls and DKD patients. (**A**) Representative immunohistochemical analysis of SPP1 and CD44 staining in healthy controls and DKD patients. Brown staining indicates the protein expression of SPP1 and CD44. Scale bar =50 μm; (**B**) Quantification of SPP1 immunohistochemical staining (n=8 in each group); (**C**) Quantification of CD44 immunohistochemical staining (n=8 in each group). *$P<0.05$, **$P<0.005$, ****$P<0.0001$.

glomeruli, especially in the renal tubule. The growth of plasma cells, monocytes, and M1 macrophages was also observed in the renal tubules. Some of which are consistent with previous reports. For example, Guiteras R et al found that the kidney displayed high CD86+/F4/80+ macrophages and CD40 expression in diabetic animals compared to healthy controls.[17] Fu J et al focused on the changes in specific macrophage cell subsets in early DKD and found that over time, the infiltration of macrophage subsets and the M1-like inflammatory phenotype in the kidney of diabetic mice gradually increased.[18] However, a cross-sectional study from seven communities in China reported that no significant correlation was found between peripheral blood monocyte levels and the prevalence of DKD, whereas the changes in monocyte levels in renal tissue are still unclear.[19]

With the development of bioinformatics, single cell sequencing gives us a recency perspective to understand the pathophysiology of disease one step forwards. Two scRNA datasets were obtained, and meticulous cell clustering was carried out based on marker genes. The immune cells in DKD had an approximate 7- to 8-fold increase compared to controls, which is consistent with previous reports. We then predicted the interaction between different immune cells and renal innate cells, especially podocytes, PCTs, and In. PCTs in DKD. Compared with control groups, VISFATIN, GALECTIN, and CSF signaling patterns increased in monocytes, with CXCL, IGF, and GALECTIN rising in T cells in the human DKD samples. Meanwhile, in mice db/db samples, IGF, CSF, TGF-β, and GALECTIN signaling patterns increased in macrophages, with FGF, GDF and GALECTIN rising in T cells. As the signaling pathway with the most frequent occurrence, galectins belong to carbohydrate-binding proteins and are considerable regulators of immunological homeostasis and immune responses. Galectin-3, for example, could enhance immune responsiveness and the inflammatory cascade.[20] Hussain et al have reported that galectin-3 was significantly increased in type 2 diabetes mellitus (T2DM) patients with macroalbuminuria and poor kidney function, which might become the early detection indicator of DKD.[21] Colony stimulating factor (CSF) is one of the most common proinflammatory cytokines responsible for various inflammatory disorders.[22] Brandt S et al found that the expression of CSF and the interaction between CSF and CSF receptors were enhanced with severe renal function in CKD, and inhibition of the interaction had a protective role on the

kidney. In contrast, the secretion of CSF in renal tubules had a significant protective effect on the kidney in AKI, which was related to the CSF-mediated transformation of infiltrating monocytes into M2-type macrophages.[23] Visfatin is an adipocytokine and could induce proinflammatory cytokines production and inhibit insulin signaling via increasing the activities of the JAK2/STAT3 and IKK/NF-κB signaling pathways.[24]

Kacso A. C et al reported that visfatin was positively linked to C-creative protein (CRP) and leukocytes in patients with DKD, and the main connection of visfatin with DKD is inflammation.[25] We found that visfatin pathway associated with monocytes was significantly enhanced in DKD and had a stronger signaling sender and influencer function, suggesting that inflammatory signals might be sent to renal innate cells through visfatin. The insulin-like growth factor (IGF) system includes receptors for IGF-1, IGF-2, and insulin, etc.[26] Li J et al reported that IGF-1/IGF-1R expression was significantly increased, and inhibition of IGF-1R was an effective method to reduce urinary protein excretion rate and inflammatory infiltration in DKD model induced by high-fat diet and intraperitoneal administration of streptomycin.[27] It was further confirmed that inhibition of IGF-1R could ameliorate the hypertrophy of glomeruli, infiltration of inflammatory cells, and fibrosis of renal tubule interstitium at the cellular level, which might be related to the down-regulation of activated Snail1.[28] In this study, the sender and influencer role of macrophages was significantly enhanced in IGF pathways. PCTs still acted as the main receiver in the mice datasets, suggesting that macrophages might send IGF signals to participate in the inflammation process and proximal tubule cells injury during DKD.

Receptor ligand pairs behind the signaling pathway demonstrated above were further explored in detail. PLG-PARD3, SPP1-CD44, SPP1-(ITGA9+ITGB1), NRG1-ERBB4, and NAMPT-INSR were identified as essential bridges between T cells, monocytes, and PCTs in human datasets. For example, Osteopontin (OPN), encoded by SPP1, could bind with its mutual cell surface receptor CD44.[29] The N-terminal fragment of osteopontin (N-OPN), carried by the exosome, could promote fibroblast proliferation and activation through binding with CD44 in the urine of CKD patients, which was negatively correlated with renal function.[30] Neuregulin-1 (NRG1) is a member of the polypeptide growth factor family, which combines with the ErbB family of receptor protein tyrosine kinases, phosphorylates and dimerizes the latter, consequently activating the downstream signaling pathways and was involved in cell survival, migration, proliferation, and differentiation.[31] NRG1-ErbB4-C/EBPβ and IGF-1-PI3k-Akt signaling pathways are associated with exercise-related cellular adaptations.[32] As the role of macrophages in type 2 DKD is well documented, Sema3g-(Nrp1+Plxna4), Gas6-Mertk, Nrg2-Erbb3, and Igf1- Igf1r receptor ligand pairs were similarly found in the interaction of PCTs and macrophages by analysis of mice datasets. Semaphorin 3G (Sema3G) belongs to the semaphorin family and is identified as one of the glomerulus-specific transcripts. The Sema3G protein is secreted by podocytes and could protect podocytes from inflammatory insult and diabetic nephropathy.[33] However, the specific mechanism of these receptor ligand pairs is still not studied enough under DKD conditions. Using the Nephroseq v5 online tool, we found that the mRNA expression of NRG1, PLG, PARD3, and SEMA3G were positively correlated with GFR, with SPP1 and IGF1 negatively correlated. Taken together, These findings provided new potential targets for future DKD treatment.

Conclusion

In conclusion, our current study analyzed immune cells and inflammation-related pathways in DKD, further revealing that VISTANT, SPP1, GALECTIN and IGF signaling pathways and SPP1-CD44, NRG1-ERBB4, NAMPT-INSR, Sema3g (Nrp1+Plxna4), Igf1- Igf1r receptor ligand pairs might occupy an important place in the occurrence and progress of DKD. The corresponding specific mechanisms need to be further improved and verified.

Ethics Approval and Informed Consent

All experiments and methods were performed in accordance with relevant guidelines and regulations. This study protocol was reviewed and approved by the Ethics Committee of the First Affiliated Hospital of Nanjing Medical University. Informed consent was obtained from all individual participants included in the study. We strictly abided the principles of the Declaration of Helsinki.

Acknowledgments

Disclosure

The authors declare that they have no competing interests.

References

1. Sinclair A, Saeedi P, Kaundal A, et al. Diabetes and global ageing among 65-99-year-old adults: findings from the international diabetes federation diabetes atlas. *Diabetes Res Clin Pract*. 2020;162:108078. doi:10.1016/j.diabres.2020.108078

2. Reutens AT. Epidemiology of diabetic kidney disease. *Med Clin North Am*. 2013;97(1):1–18. doi:10.1016/j.mcna.2012.10.001

3. Crews DC, Bello AK, Saadi G. Burden, access, and disparities in kidney disease. *Blood Purif*. 2019;48(1):32–39. doi:10.1159/000497498

4. Sagoo MK, Gnudi L. Diabetic nephropathy: an overview. *Methods Mol Biol*. 2020;2067:3–7.

5. Lin YC, Chang Y-H, Yang S-Y, et al. Update of pathophysiology and management of diabetic kidney disease. *J Formos Med Assoc*. 2018;117 (8):662–675. doi:10.1016/j.jfma.2018.02.007

6. Alicic RZ, Rooney MT, Tuttle KR. Diabetic kidney disease: challenges, progress, and possibilities. *Clin J Am Soc Nephrol*. 2017;12 (12):2032–2045. doi:10.2215/CJN.11491116

7. Samsu N, Bellini MI. Diabetic nephropathy: challenges in pathogenesis, diagnosis, and treatment. *Biomed Res Int*. 2021;2021:1497449. doi:10.1155/2021/1497449

8. Doshi SM, Friedman AN. Diagnosis and management of type 2 diabetic kidney disease. *Clin J Am Soc Nephrol*. 2017;12(8):1366–1373. doi:10.2215/CJN.11111016

9. Jia Y, Xu H, Yu Q, et al. Identification and verification of vascular cell adhesion protein 1 as an immune-related hub gene associated with the tubulointerstitial injury in diabetic kidney disease. *Bioengineered*. 2021;12(1):6655–6673. doi:10.1080/21655979.2021.1976540

10. Kauffmann A, Gentleman R, Huber W. arrayQualityMetrics–a bioconductor package for quality assessment of microarray data. *Bioinformatics*. 2009;25(3):415–416. doi:10.1093/bioinformatics/btn647

11. McGinnis CS, Murrow LM, Gartner ZJ. DoubletFinder: doublet detection in single-Cell RNA sequencing data using artificial nearest neighbors. *Cell Syst*. 2019;8(4):329–337.e4. doi:10.1016/j.cels.2019.03.003

12. Butler A, Hoffman P, Smibert P, et al. Integrating single-cell transcriptomic data across different conditions, technologies, and species. *Nat Biotechnol*. 2018;36(5):411–420. doi:10.1038/nbt.4096

13. Zhang X, Lan Y, Xu J, et al. CellMarker: a manually curated resource of cell markers in human and mouse. *Nucleic Acids Res*. 2019;47(D1):D721–d728. doi:10.1093/nar/gky900

14. Ritchie ME, Phipson B, Wu D, et al. limma powers differential expression analyses for RNA-sequencing and microarray studies. *Nucleic Acids Res*. 2015;43(7):e47. doi:10.1093/nar/gkv007

15. Ashburner M, Ball CA, Blake JA, et al. Gene ontology: tool for the unification of biology. The Gene Ontology Consortium. *Nat Genet*. 2000;25 (1):25–9. doi:10.1038/75556B1

16. Kanehisa M, Goto S. KEGG: kyoto encyclopedia of genes and genomes. *Nucleic Acids Res*. 2000;28(1):27–30. doi:10.1093/nar/28.1.27B2

17. Guiteras R, Sola A, Flaquer M, et al. Exploring macrophage cell therapy on diabetic kidney disease. *J Cell Mol Med*. 2019;23(2):841–851. doi:10.1111/jcmm.13983

18. Fu J, Sun Z, Wang X, et al. The single-cell landscape of kidney immune cells reveals transcriptional heterogeneity in early diabetic kidney disease. *Kidney Int*. 2022;102:1291–1304. doi:10.1016/j.kint.2022.08.026

19. Wan H, Cai Y, Wang Y, et al. The unique association between the level of peripheral blood monocytes and the prevalence of diabetic retinopathy: a cross-sectional study. *J Transl Med*. 2020;18(1):248. doi:10.1186/s12967-020-02422-9

20. Johannes L, Jacob R, Leffler H. Galectins at a glance. *J Cell Sci*. 2018;131(9). doi:10.1242/jcs.208884

21. Hussain S, Habib A, Hussain MS, et al. Potential biomarkers for early detection of diabetic kidney disease. *Diabetes Res Clin Pract*. 2020;161:108082. doi:10.1016/j.diabres.2020.108082

22. Kumari A, Silakari O, Singh RK. Recent advances in colony stimulating factor-1 receptor/c-FMS as an emerging target for various therapeutic implications. *Bio Pharmacot*. 2018;103:662–679. doi:10.1016/j.biopha.2018.04.046

23. Brandt S, Mertens PR. The kidney regulates regeneration, but don't upset the balance. *Int Urol Nephrol*. 2016;48(8):1371–1376. doi:10.1007/s11255-016-1302-3

24. Heo YJ, Choi S-E, Jeon JY, et al. Visfatin induces inflammation and insulin resistance via the NF-κB and STAT3 signaling pathways in hepatocytes. *J Diabetes Res*. 2019;2019:4021623. doi:10.1155/2019/4021623

25. Kacso AC, Bondor CI, Coman AL, et al. Determinants of visfatin in type 2 diabetes patients with diabetic kidney disease: relationship to inflammation, adiposity and undercarboxylated osteocalcin. *Scand J Clin Lab Invest*. 2016;76(3):217–225. doi:10.3109/00365513.2015.1137349

26. Rae FK, Suhaimi N, Li J, et al. Proximal tubule overexpression of a locally acting IGF isoform, Igf-1Ea, increases inflammation after ischemic injury. *Growth Horm IGF Res*. 2012;22(1):6–16. doi:10.1016/j.ghir.2011.11.002

27. Li J, Dong R, Yu J, et al. Inhibitor of IGF1 receptor alleviates the inflammation process in the diabetic kidney mouse model without activating SOCS2. *Drug Des Devel Ther*. 2018;12:2887–2896. doi:10.2147/DDDT.S171638

28. Dong R, Yu J, Yu F, et al. IGF-1/IGF-1R blockade ameliorates diabetic kidney disease through normalizing Snail1 expression in a mouse model. *Am J Physiol Endocrinol Metab*. 2019;317(4):E686–e698. doi:10.1152/ajpendo.00071.2019

29. Asselman M, Verhulst A, de Broe ME, et al. Calcium oxalate crystal adherence to hyaluronan-, osteopontin-, and CD44-expressing injured/regenerating tubular epithelial cells in rat kidneys. *J Am Soc Nephrol*. 2003;14(12):3155–3166. doi:10.1097/01.ASN.0000099380.18995.F7

30. Chen S, Zhang M, Li J, et al. β-catenin-controlled tubular cell-derived exosomes play a key role in fibroblast activation via the OPN-CD44 axis. *J Extracell Vesicles*. 2022;11(3):e12203. doi:10.1002/jev2.12203

31. Wu L, Walas SJ, Leung W, et al. *Frontiers in Neuroengineering Neuregulin-1 and Neurovascular Protection, in Brain Neurotrauma: Molecular, Neuropsychological, and Rehabilitation Aspects*. Boca Raton (FL): CRC Press/Taylor & Francis© 2015 by Taylor & Francis Group, LLC; 2015.

32. Tao L, Bei Y, Zhang H, et al. Exercise for the heart: signaling pathways. *Oncotarget*. 2015;6(25):20773–20784. doi:10.18632/oncotarget.4770

33. Ishibashi R, Takemoto M, Akimoto Y, et al. A novel podocyte gene, semaphorin 3G, protects glomerular podocyte from lipopolysaccharide-induced inflammation. *Sci Rep*. 2016;6:25955. doi:10.1038/srep25955